

Micromechanical analysis for evaluation of voids effect on thermoelastic properties of composites via 1D higher-order theories

Rebecca Masia^{1, a *}

¹Department of Mechanical and Aerospace Engineering, Politecnico di Torino, 10129, Torino, Italy

^arebecca.masia@polito.it

Keywords: Micromechanics, Voids, CUF, RVE, Composite Materials, Statistical Analysis

Abstract. The present work presents statistical results of numerical simulations to investigate the effect of different void percentages on composite materials' coefficient of thermal expansion (CTE). A random distribution of voids is simulated over the Representative Volume Element (RVE) matrix. The use of a high-order beam model within the framework of Carrera Unified Formulation (CUF) leads to a Component Wise (CW) description of the model cross-section. Numerical results for different fiber volume fractions and void concentration percentages are carried out, and the comparison with references from literature demonstrates the agreement in the average CTE trend.

Introduction

Fiber-reinforced composites have proven to have excellent thermo-mechanical properties such as lightweight, mechanical performance at high temperature and good thermal stability. The coefficient of thermal expansion (CTE) plays a critical role in designing composite materials since it can directly determine the dimensional stability of the structure and thermal stress distribution. Moreover, the multiscale nature of composites requires the development of accurate multiscale models. Another critical aspect is the growth of defects that inevitably occur during the manufacturing process. Specifically, voids are the primary manufacturing defects that significantly influence thermal properties, and this influence needs to be investigated.

Most of the numerical simulations for the homogenization analysis usually employ Representative Volume Element (RVE) models, which represent the smallest geometric entity containing all the information about material properties and volume fraction of the constituents. Many numerical and analytical approaches are available for obtaining homogenized properties. For instance, in [1], the Mechanics of Structure Genome (MSG) coupled with Carrera Unified Formulation (CUF) and Hierarchical Legendre Expansions (HLE) for the discretization of the cross-section allows the computation of thermo-elastic properties of a Repeatable Unit Cell (RUC) model. Another MSG-based analysis computes the CTE of solid models [2]. Finally, in [3], semi-analytical models for the computation of homogenized CTE are presented, such as the High Fidelity Generalized Method of Cells (HFGMC).

The present article adopts the CUF to obtain a one-dimensional (1D) high-order Finite Element Method (FEM) analysis reducing the computational costs while maintaining 3D accuracy of the model. Hence, shape functions act along the RVE axis, and expansion functions enhance the cross-section kinematics.

The aim of the present work is to investigate the influence of microscale matrix voids on the prediction of effective CTEs of RVE models with different percentages of void and fiber volume fractions.

This work is organized as follows: Section 2 presents the high-order theory formulation; Section 3 introduces the micromechanics model; Section 4 provides numerical results and their discussion; and the conclusions are given in Section 5.

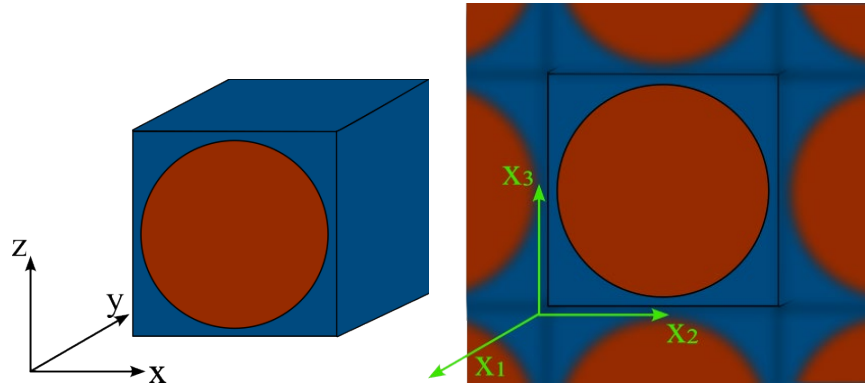


Figure 1 Square-pack RVE model with reference system high-order theory (left), and reference frame in micromechanics (right).

High-order beam theory

The present work exploits the capabilities of a refined 1D kinematic model. The three components of the displacement field are defined according to the reference system in Fig. 1

$$u(x, y, z) = \{u_x \ u_y \ u_z\}^T \quad (1)$$

The governing equations of the problem have been derived within the CUF framework [4]. Therefore, the displacement field becomes:

$$u(x, y, z) = F_\tau(x, z)u_\tau(y), \quad \tau = 1, 2, \dots, M \quad (2)$$

where $F_\tau(x, z)$ are the expansion functions employed over the cross-section, u_τ is the vector of general displacement and M is the number of terms in the expansion. In addition, τ denotes the summation of the expansion terms. Lagrange polynomials have been employed as expansion functions, leading to a Component Wise (CW) approach. By describing the longitudinal direction according to the finite element method (FEM), shape functions are introduced:

$$u(x, y, z) = F_\tau(x, z)N_i(y)u_{\tau i}, \quad \tau = 1, 2, \dots, M, \quad i = 1, 2, \dots, p + 1 \quad (3)$$

where $N_i(y)$ represents the shape functions of p order and $u_{\tau i}$ is the vector of nodal displacements. The stress vector is defined as:

$$\sigma^T = \{\sigma_{xx} \ \sigma_{yy} \ \sigma_{zz} \ \sigma_{xy} \ \sigma_{xz} \ \sigma_{yz}\} \quad (4)$$

The geometrical equation is involved as relation between strains and displacements:

$$\varepsilon = D u \quad (5)$$

where D is the 6×3 differential operator. Then, the Hooke's law allows the relation between strain and stress to be defined as:

$$\sigma = C \varepsilon \quad (6)$$

where C is the stiffness matrix of the material. The governing equations are derived from the Principles of Virtual Displacement (PVD). For the static analysis the PVD can be expressed as:

$$\delta L_{int} = \delta L_{ext} \tag{7}$$

where δL_{int} is the strain energy and L_{ext} is the work of the external forces. δ is used to indicate the virtual variation of the quantity. After some mathematical steps, the strain energy can be expressed as:

$$\delta L_{int} = \delta \mathbf{u}_{sj}^T \mathbf{k}_{ij\tau s} \mathbf{u}_{\tau i} \tag{8}$$

where the explicit form of the 3×3 Fundamental Nucleus (FN) $\mathbf{k}_{ij\tau s}$ is:

$$\mathbf{k}_{ij\tau s} = \int_V N_j F_s \mathbf{D}^T \mathbf{C} \mathbf{D} N_i F_\tau dV \tag{9}$$

The external load can be expressed as:

$$\delta L_{ext} = \delta \mathbf{u}_{sj}^T \mathbf{P}_{sj} \tag{10}$$

where \mathbf{P}_{sj} is the 3×1 external load vector and is referred to as the FN of the load vector. The global stiffness matrix and the external load vector are assembled by iterating the indices i, j, τ, s . The first two indexes i, j denote the loop on the FEM nodes, while τ, s are the loop indices on the cross-section nodes.

Micromechanics formulation

The present work uses a micromechanical analysis to compute the effective thermo-elastic properties, particularly the Coefficient of Thermal Expansion (CTE) of composite materials.

The study makes use of different RVE models. The cross-section of the 1D models, illustrated in Fig. 1, is discretized with 9-node bi-quadratic elements (L9), whereas along x_1 direction two 4-nodes quadratic elements are employed. The repeatability of the model in space is guaranteed by the application of Periodic Boundary Condition (PBC), according to the reference micromechanics frame in Fig. 1.

$$u_i^{j+}(x, y, z) - u_i^{j-}(x, y, z) = \bar{\varepsilon}_{ik} \Delta x_k^j, \quad \Delta x_k^j = x_k^{j+} - x_k^{j-} \tag{11}$$

$j+$ and $j-$ indicate the positive and negative direction of the x_k and $\bar{\varepsilon}_{ik}$ is the macroscopic strain vector. The thermo-elastic analysis considers the stress field given both from the elastic and thermal contributions:

$$\sigma_{ij} = \sigma_{ij}^E + \sigma_{ij}^T \tag{12}$$

where E stands for elastic and T the thermal. The present homogenization procedure first involves the resolution of the static problem in order to obtain the effective stiffness matrix, which is then employed in the effective CTE vector.

In the micromechanics framework, the local solutions, such as the strain and stress vectors, have an average value over the RVE volume. The local elastic stress field σ_{ij}^E is defined in Eq. (6), and its macroscopic value $\bar{\sigma}_{ij}^E$ can be expressed as follows:

$$\bar{\sigma}_{ij}^E = \frac{1}{V} \int_V \sigma_{ij}^E dV \tag{13}$$

in the same way, the macroscopic strain vector is:

$$\bar{\varepsilon}_{ij}^E = \frac{1}{V} \int_V \varepsilon_{ij}^E dV \quad (14)$$

The micromechanics formulation for the elastic analysis can be deepened in [5].

Now, the effective elastic coefficients matrix \bar{C}_{ijkl} can be easily retrieved from:

$$\bar{\sigma}_{ij}^E = \bar{C}_{ijkl} \bar{\varepsilon}_{ij}^E \quad (15)$$

The local stress field given by the thermal contribution due to the application of a temperature variation θ is:

$$\sigma_{ij}^T = \beta_{ij} \theta \quad (16)$$

where $\beta_{ij} = -C_{ijkl} \alpha_{ij}$ is the local thermal induced stress vector.

Note that the temperature field applied to the RVE, unlike the stress and strain, is assumed to be uniform in the entire heterogeneous material.

By applying the integral over the volume of the thermal stress vector, it is possible to find the homogenized value $\bar{\sigma}_{ij}^T$ as done in Eq. 13. Then, by explicating Eq. 16 for β_{ij} and exploiting the relationship between β_{ij} , $\bar{\alpha}_{ij}$ and \bar{C}_{ijkl} , the effective CTE vector can be obtained by rearranging the following relation:

$$\bar{\sigma}_{ij}^T = -\bar{C}_{ijkl} \bar{\alpha}_{ij} \theta \quad (17)$$

More details about the CUF micromechanics framework are available in [6]. The voids are modeled as randomly distributed over the RVE matrix phase, according to the void volume selected for the analysis. It is considered an implicit presence of voids by assigning negligible isotropic elastic properties and a CTE equal to zero to the Gauss points associated with the single void.

Numerical results

The numerical assessments of the current work are conducted to demonstrate the reliability of the numerical simulations in computing the homogenized thermo-elastic properties of composite materials employing RVE models. In detail, the variation of the effective CTE due to the gradually enhance of the void fraction is investigated. For the sake of clarity, for each void percentage within the matrix, 100 random distributions are generated, thus requiring a statistical investigation of the results.

Influence of fiber volume fraction and void percentage on the effective CTE

An hexagonal-pack model, showed in Fig. 2, is employed for the current assessment, and two values of fiber volume fraction are evaluated. The results are compared with those reported in [7]. The material is a C/C composite in which the fiber is assumed orthotropic with $\alpha_{11} = -1 \cdot 10^{-6} [K^{-1}]$ and $\alpha_{22} = 1.8 \cdot 10^{-5} [K^{-1}]$, while the isotropic matrix has a CTE of $4 \cdot 10^{-6} [K^{-1}]$. First, the results with 0 % of voids are produced and listed in Table 1.

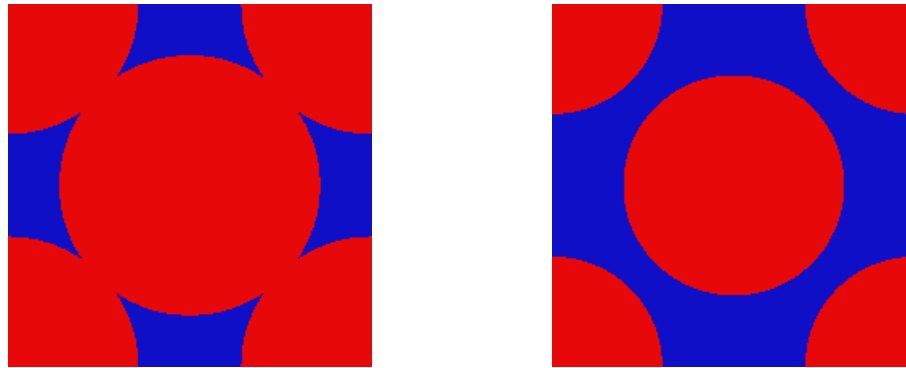


Figure 2 Hexagonal-pack model for 80% (left) and 57% (right) of fiber volume fraction.

Table 1 Effective CTEs of an hexagonal-pack model with 80% and 57% of fiber volume fraction and 0% of voids.

| Model | $\alpha_{11} \times 10^6 [K^{-1}]$ | $\alpha_{22} = \alpha_{33} \times 10^6 [K^{-1}]$ |
|------------------------|------------------------------------|--|
| | | $V_f = 57\%$ |
| Reference [7] | -0.900 | 12.720 |
| Current CUF simulation | -0.909 | 13.082 |
| | | $V_f = 80\%$ |
| Reference [7] | -0.962 | 16.450 |
| Current CUF simulation | -0.972 | 15.820 |

As expected, the longitudinal CTE decreases when the V_f rises from 57% to 80% since the fiber becomes the prevailing phase. At the same time, the transverse CTE increases with a higher value of V_f .

The following numerical instances examine the effects of void volume fraction and the fiber reinforcement phase on the effective CTE of composites. In order to understand the way the existence of voids within the material matrix affects the thermo-elastic property, void percentages between 2 and 8% are considered with 80% of fiber volume fraction. The analysis results are presented in Fig. 3.

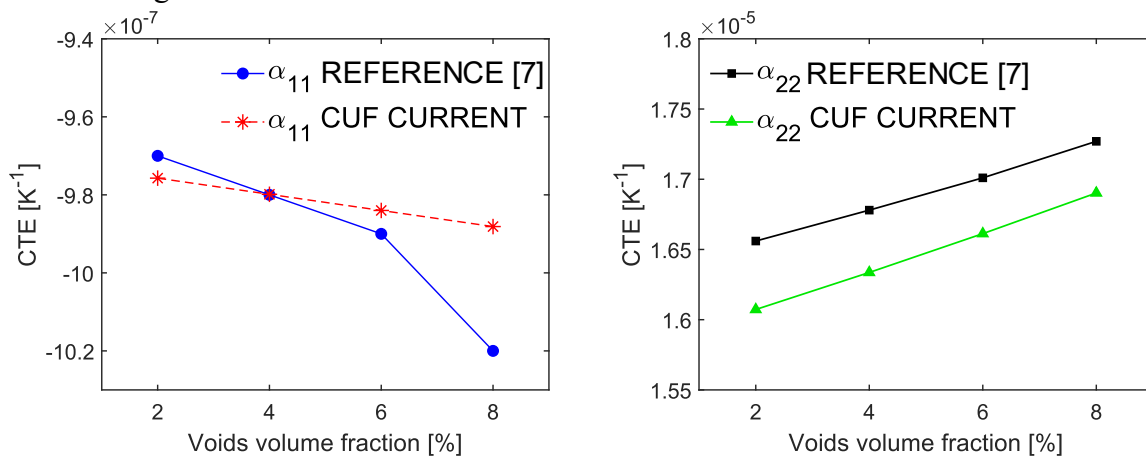


Figure 3 Variation of the longitudinal (left) and transverse (right) CTE according to the percentage voids volume fraction for the present and the reference results in [7], with 80% of fiber volume fraction.

The longitudinal CTE gradually weakens when the void volume fraction rises, while the transverse CTE tends to increase. This behavior is in agreement with evidence existing in the

literature. It may be explained by considering that when the void inclusions occur within the matrix, the contribution of a low fiber CTE and the zero value of void CTE make obvious the collapse of the effective CTE along the longitudinal direction. Conversely, when the RVE transverse direction is considered, the rise in void percentage within the matrix makes the transverse CTE of the fiber the most impactful contribution in that direction. Indeed, it can be noticed that as the void fraction increases, the overall CTE tends to be closer to the cross-sectional CTE of the fiber. In Fig. 4, the percentage variation of α_{11} and α_{22} is shown. The calculation assumes the relative CTE with 0% voids of the reference solution in [7].

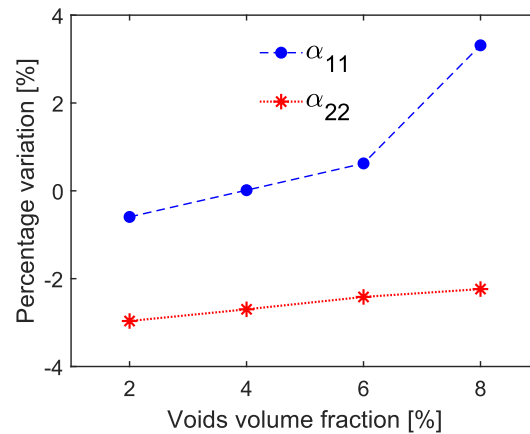


Figure 4 Percentage of the relative variation of longitudinal and transverse CTE between the present and the reference results in [7].

Fig. 4 highlights the discrepancies between the two methods with the decreasing of CTE value. Considering the transversal CTE, the values tend to be closer when higher void concentration occurs.

Conclusions

The present study investigated the effect of random distribution of voids within the matrix phase of composites on the effective coefficient of thermal expansion (CTE) for different Representative Volume Elements (RVE) models and fiber volume fractions. The homogenization analysis is conducted in the micromechanics framework, in which the use of the Carrera Unified Formulation (CUF) allows a Component Wise (CW) approach. The statistical analysis led to detect mean values of outcomes, thus minimizing the influence of the void distribution. A square-pack and a hexagonal-pack RVE with different fiber volume fractions are involved in the investigation. Periodic Boundary Conditions (PBC) ensured the periodicity constraint imposed by micromechanics analyses. The results demonstrated that manufacturing defects might increase or decrease the homogenized CTEs. Future investigations will focus on extending the study to the dehomogenization procedure to investigate localized stress and strain fields over the RVE volume for different void percentages and cluster distribution.

Acknowledgements

This work is part of a project that has received funding from the European Research Council (ERC) under the European Union’s Horizon 2020 research and innovation programme (Grant agreement No. 850437). The author would also like to thank Mattia Trombini for the collaboration with the analysis of the outcomes.

References

[1] A. R. Sanchez-Majano, R. Masia, A. Pagani, E. Carrera. Microscale thermo-elastic analysis of composite materials by high-order geometrically accurate finite elements, Composite Structures, 2022, Vol. 300, p. 116105. <https://doi.org/10.1016/j.compstruct.2022.116105>

- [2] X. Liu, W. Yu, F. Gasco, J. Goodsell. A unified approach for thermoelastic constitutive model of composite structures, *Composites Part B*, 2019, Vols. 172:649-59.
<https://doi.org/10.1016/j.compositesb.2019.05.083>
- [3] J. Aboudi, S. M. Arnold, and B. A. Bednarczyk. *Practical Micromechanics of Composite Materials*, 1st Edition, Butterworth-Heinemann, Oxford Spire Business Park, Kidlington, Oxfordshire, United Kingdom, 2021.
- [4] E. Carrera, M. Cinefra, M. Petrolo, E. Zappino. *Finite element analysis of structures through unified formulation*. John Wiley & Sons, 2014. <https://doi.org/10.1002/9781118536643>
- [5] E. Carrera, M. Petrolo, M.H. Nagaraj, M. Delicata. Evaluation of the influence of voids on 3D representative volume elements of fiber-reinforced polymer composites using CUF micromechanics. *Composite Structures*, 2020, Vol. 254.
<https://doi.org/10.1016/j.compstruct.2020.112833>
- [6] I. Kaleel, M. Petrolo, E. Carrera, A. M. Waas, *Computationally Efficient Concurrent Multiscale Framework for the Linear Analysis of Composite Structures*. *AIAA Journal*, 2019, Vol. 57(9). <https://doi.org/10.2514/1.J057880>
- [7] K.L. Wei, J. Li, H.B. Shi, M. Tang. Numerical evaluation on the influence of void defects and interphase on the thermal expansion coefficients of three-dimensional woven carbon/carbon composites. 2020, *Composite Interfaces*, Vol. 27, pp. 873-892.
<https://doi.org/10.1080/09276440.2019.1707586>